One-year records of current and bottom pressure in the strait between Nordaustlandet and Kvitøya, Svalbard, 1980–81

K. AAGAARD, A. FOLDVIK, T. GAMMELSRØD AND T. VINJE

We have obtained one year of measurements from a subsurface instrumented mooring carrying two current meters and one bottom pressure recorder in the strait between Nordaustlandet and Kvitøya in the northeastern Svalbard archipelago. The observations show a mixed tide with typical amplitudes 0.4 db and 10 cm sec^{-1}. The semidiurnal tide is characterized by a progressive wave propagating toward the south, together with a cross-channel baroclinic mode. The annual average (non-tidal) current is less than 2 cm sec^{-1} toward the north-east, suggesting that the transport into the Arctic Ocean is approximately 0.2×10^6 m^3 s^{-1}.

K. Aagaard, University of Washington, 4057 Roosevelt Way, N.E. Seattle, Washington 98105, U.S.A.; A. Foldvik and T. Gammelsrød, Geofysisk Institutt, Avd. A, Universitetet i Bergen, 5014 Bergen, Norway; T. Vinje, Norsk Polarinstitutt, Rolfstangveien 12, 1330 Oslo Lufthavn, Norway; December 1982 (revised February 1983).

Introduction

In this paper we present the results from a subsurface mooring between Kvitøya and Nordaustlandet in the northeastern Svalbard archipelago (Fig. 1). The rig was launched from the Swedish icebreaker YMER on 30 July 1980 and recovered from the Norwegian vessel LANCE on 25 August 1981. It consisted of two Aanderaa RCM-4 current meters at 75 m and 255 m, and one Aanderaa
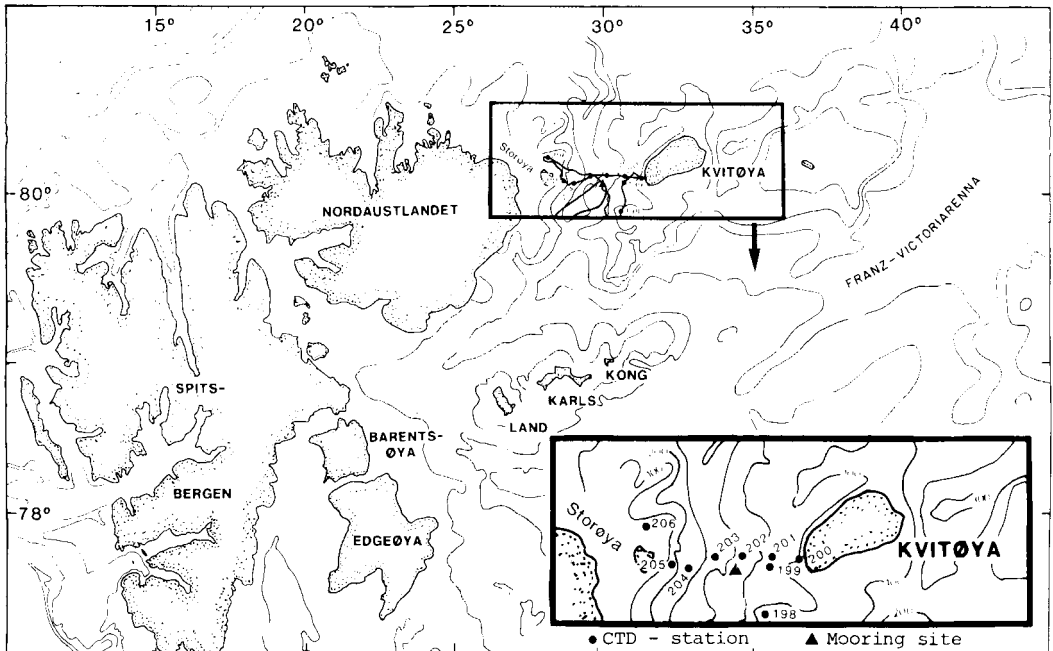
Fig. 1. Map of Svalbard showing positions of mooring and CTD section.
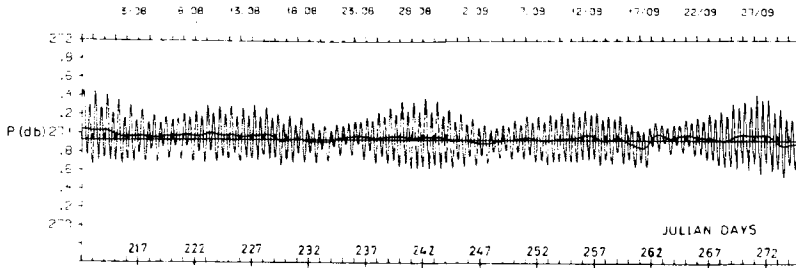
Fig. 2. Hourly bottom pressure from August to September 1980. Time in Julian days. Also shown is the low-passed series, using a filter with a 40 hr cut-off.

TG-2A pressure recorder at the bottom (260 m). The sampling interval was one hour. An apparent deterioration in the speed recording of the lower current meter over the last 20 weeks of deployment caused the only data gap.

Pressure measurements

The bottom pressure record reflects the combined effect of variations in sea level (e.g. that due to tides), varying atmospheric pressure, and baroclinic currents. Fig. 2 shows the pressure recording for the two months immediately following the launching. A typical mixed tide prevailed, with the semidiurnal components dominating. The fortnightly period is due to the interference of the semidiurnal periods M_2 and S_2. The maximum amplitude is seen to be roughly 0.4 decibar, equivalent to 0.4 m in sea level.

Also presented in Fig. 2 is the residual pressure

after tidal variations have been filtered out using a low-pass filter which suppresses variations with periods shorter than 40 hours. The amplitude of the filtered curve is equivalent to about 10 cm and represents the combined effects of low-frequency currents and atmospheric pressure variations.

The power spectrum of the pressure record (Fig. 3) yields the expected tidal bands. The large subharmonic components which appear near 8 hr, 6 hr, etc., are typical for shallow water tides, and arise from the non-harmonic tidal wave form in shallow water. The amplitude and phase of the major tidal constituents have been computed from the entire one-year record using Foreman's (1977, 1978) method. The results are listed in Table 1.

Current and temperature measurements

Fig. 4 shows a temperature, salinity, and density section across the strait two days after the recovery of the mooring. The lower current meter had been situated near the bottom in the warmest water, while the upper meter was at the position of the cold core at 75 m depth.

Portions of the various temperature and velocity records are shown in Fig. 5, covering the same period as the pressure record in Fig. 2. As with the pressure signal, the tides also dominate the currents. The amplitude and phase of the major tidal constituents have been computed using the full-length records, and the results are listed in Table 1. The V (north)-component of the upper current meter exhibits the largest amplitude, about 10 cm sec^{-1}. Power spectra of the current components (not shown) are similar to the power spectrum for the pressure record (Fig. 3).

The temperature spectra (Fig. 6) show no tidal
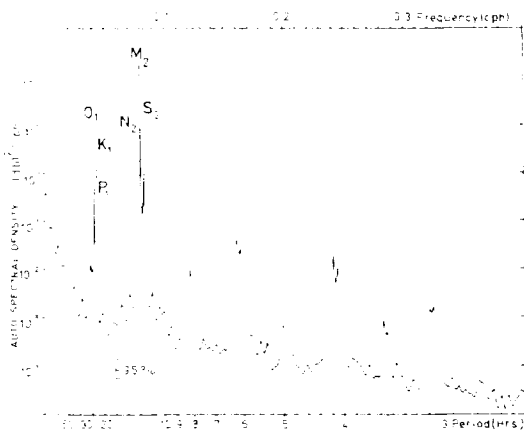
Fig. 3. The power spectrum for the entire one-year bottom pressure record, computed using the maximum entropy method. The frequencies of the major tidal constituents are also shown.

Table 1. Major tidal constituents for the upper current meter (upper numbers), the lower current meter (lower numbers) and the pressure. Positive minor axis denotes counter-clockwise rotation. The angle of inclination denotes the orientation of the major axis and is measured in degrees counter-clockwise from east. Greenwich phase is referred to the northern major semiaxis for the current and to high water for the pressure.

Constituent	Current measurements				Pressure measurements	
	Major axis cm sec^{-1}	Minor axis cm sec^{-1}	Angle of inclination degrees	Greenwich phase degrees	Amplitude decibars	Greenwich phase degrees
O_1	0.45	−0.18	147	34	0.01	320
	0.25	−0.01	158	26		
P_1	0.47	−0.00	95	68	0.02	295
	0.24	0.04	109	67		
K_1	1.29	−0.09	104	67	0.07	305
	0.88	0.16	117	68		
N_2	1.65	−0.45	89	230	0.04	68
	0.70	0.39	104	237		
M_2	8.63	−2.18	96	265	0.21	97
	3.61	2.37	102	267		
S_2	3.50	−1.32	105	337	0.06	152
	1.39	0.73	39	268		

influence other than a rather broad semidiurnal peak, probably due to a semidiurnal internal tide (see discussion below). The different spectral levels for the two instruments reflect the weaker temperature stratification in the lower layer (cf. Fig. 4).

We have applied the 40-hr filter to the entire pressure, current and temperature records; the results are shown in Fig. 7. The filtered currents are weak, about 2 cm sec^{-1}, and exceed 5 cm sec^{-1} only for short periods of time. The average flow is approximately northeast, i.e. into the Arctic Ocean, as is also apparent from the progressive vector diagrams (Fig. 8).
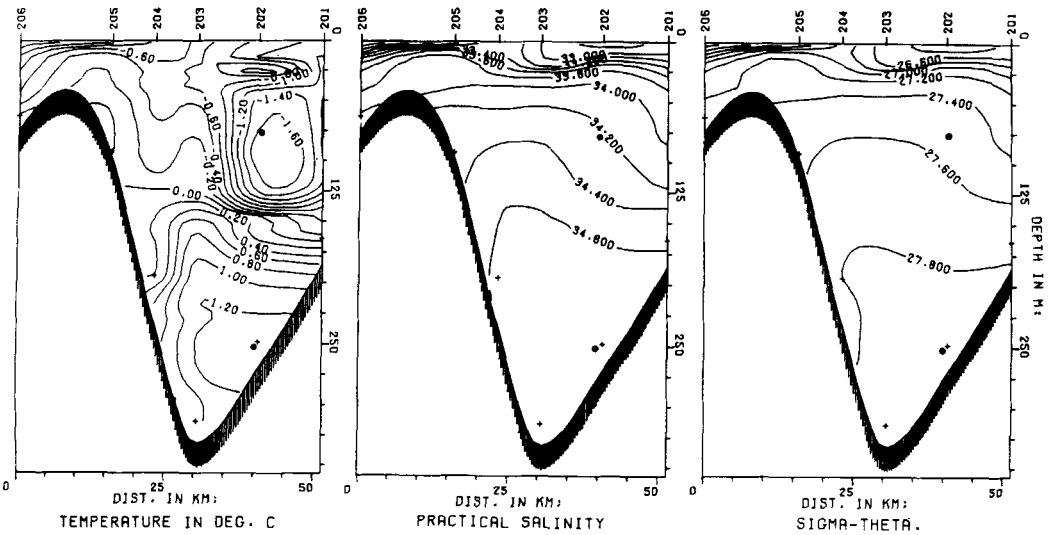
Fig. 4. A temperature, salinity and density section across the strait between Nordaustlandet and Kvitøya. The upper numbers identify the oceanographic stations. The deepest observations are marked with crosses and the positions of the current meters with black dots.
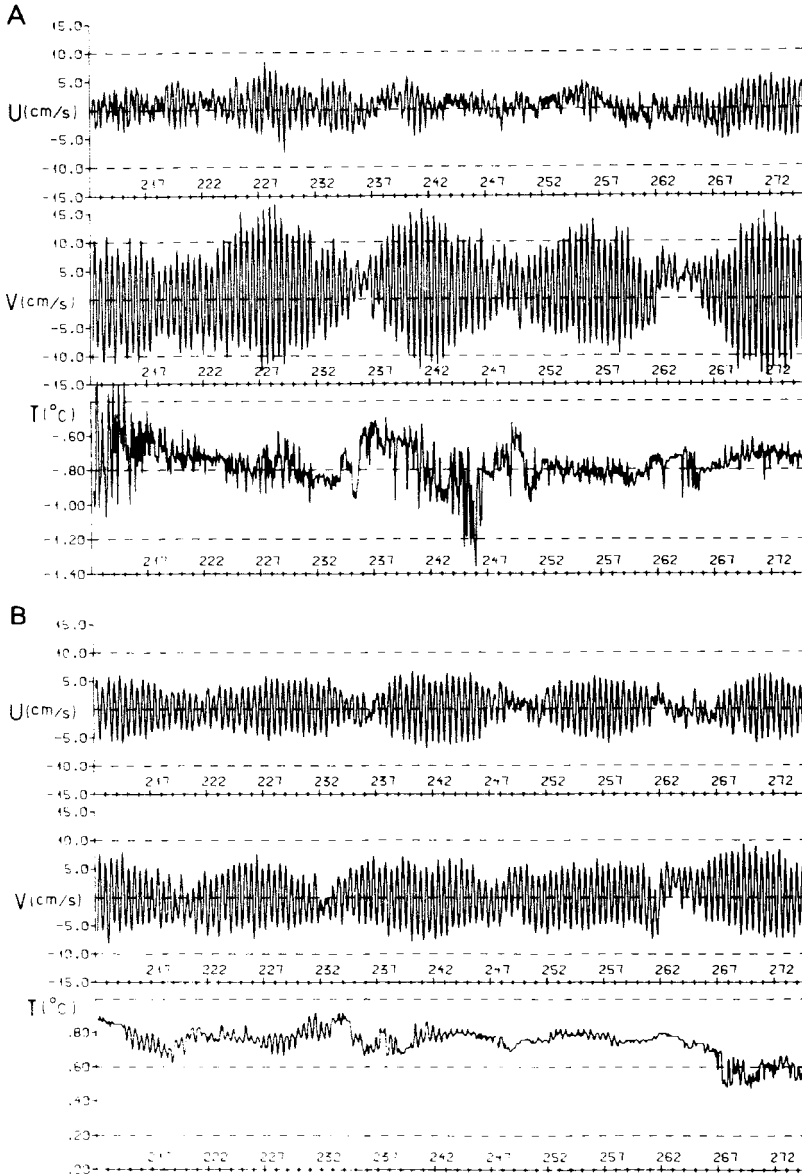
Fig. 5. Hourly current and temperature data from August to September 1980 (cf. Fig. 2). Time in Julian days. Easterly flow is denoted by U, northerly by V and temperature by T. A: Upper instrument, depth 75 m; B: Lower instrument, depth 255 m.

The average velocities in the upper and lower layers are 1.8 cm sec^{-1} and 0.5 cm sec^{-1}, respectively (the latter value was calculated up until 4 April only). From this we estimate that the annual average flow through the strait probably does not exceed about $0.2 \times 10^6 \text{m}^3 \text{sec}^{-1}$ (0.2 Sv) toward the northeast. In terms of mass balance for the Arctic Ocean, this is a small contribution (SCOR Working Group 58, 1979); for example, it is probably less than 5% of the West Spitsbergen Current transport. The temperature records (Fig. 7) show that the structure revealed in Fig. 4, with a cold core above a warm bottom layer, is maintained throughout the year.
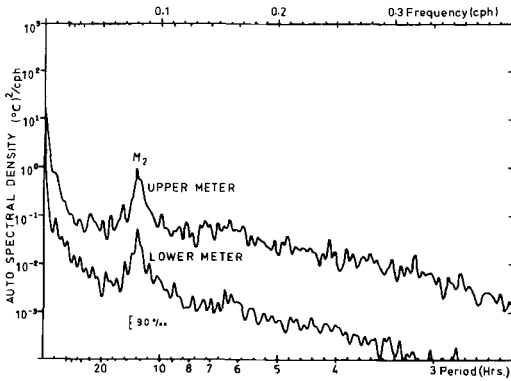
Fig. 6. Power spectra of temperature.

Discussion

Neither the filtered series themselves (Fig. 7) nor their power spectra (not shown) indicate distinct long-term periodicities. There are, however, a few events of strong northerly currents at both instruments (e.g. 28 January and 23 February, cf. Fig. 7) which coincide with anomalously high bottom pressure. On both occasions, relatively intense cyclones passed over the northern Barents Sea, and the strong current events were probably forced by the atmospheric events.

The rotary spectra for the current records are shown in Fig. 9. A comparison of the energy
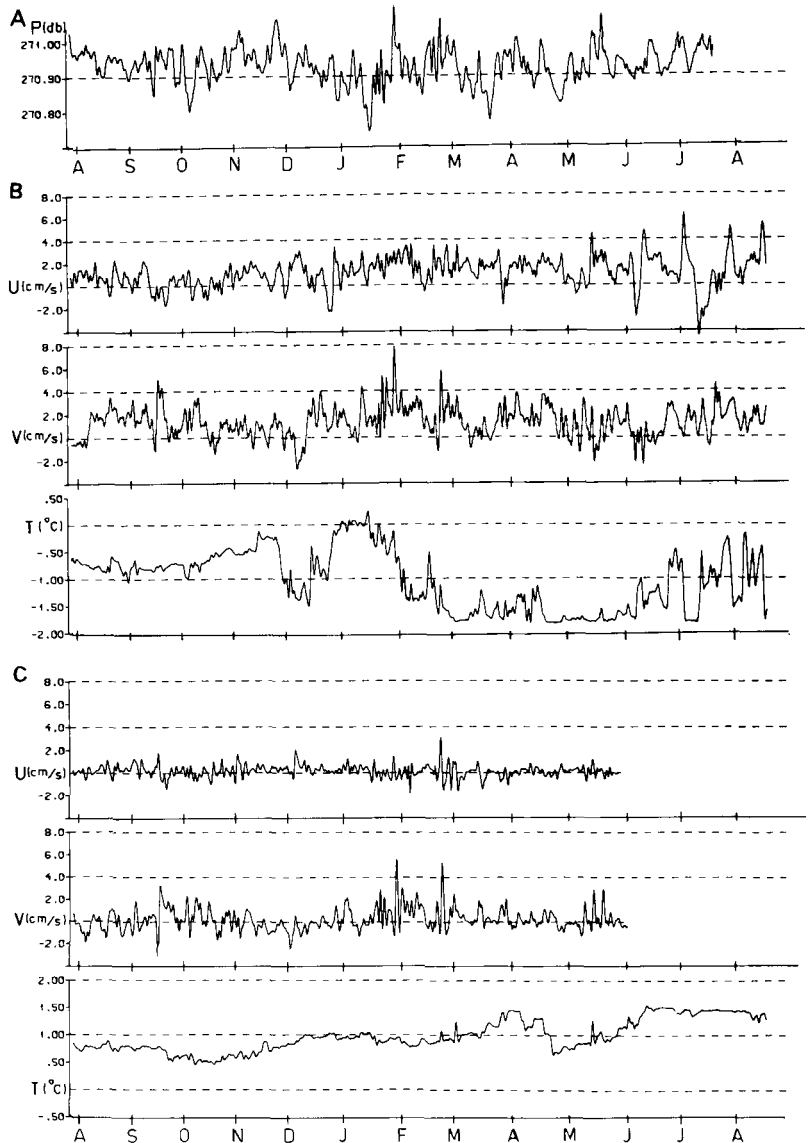
Fig. 7. Low-passed data. A: Bottom pressure; B: Velocity and temperature, upper meter; C: Velocity and temperature, lower meter.
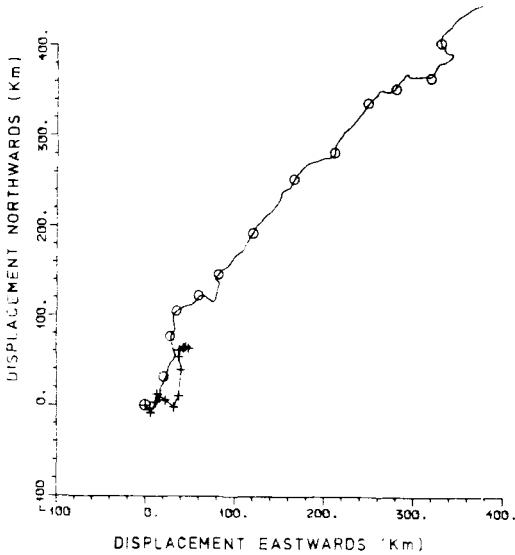
Fig. 8. Progressive vector diagram for the two current meters. Circles (upper meter) and crosses (lower meter) denote position every 30 days.

Fig. 9. Rotary current spectra. The frequencies of the major tidal constituents are indicated.

levels in the tidal bands shows that the counter-clockwise components are equal in the upper and lower layers, whereas the energy in the clockwise component is smaller at the lower instrument, particularly for the semidiurnal tide. The distribution of energy in the tidal bands also shows that the associated tidal currents rotate in opposite directions at the two instruments, clockwise in the upper layer and counter-clockwise in the lower. This is clearly seen in Fig. 10, where the tidal current ellipses are plotted; the current vectors are shown at the time of high tide. The maximum southward flow in both layers is seen to coincide with high tide. Thus the north–south tidal currents have the characteristics of southward-propagating progressive waves. A quarter period after high tide the maximum westward flow in the upper layer coincides with maximum eastward flow in the lower layer. The motion across the axis of the channel thus has the characteristics of a standing internal wave.

References

Foreman, M. G. G. 1977: Manual for Tidal Heights Analysis and Prediction. *Pacific Marine Science Report 77–10* (Corr. 1979). Institute of Ocean Sciences, Patricia Bay, Sidney, B.C.

Foreman, M. G. G. 1978: Manual for Tidal Currents. Analysis and Prediction. *Pacific Marine Science Report 78–6* (Corr. 1979). Institute of Ocean Sciences, Patricia Bay, Sidney, B.C.

SCOR Working Group 58, 1979: The Arctic Ocean Heat Budget. *Report No. 52.* Geophysical Institute, University of Bergen, Norway.

O₁   K₁   P₁

N
W ← → E
S

0 cm/s   1   2

4887 upper inst.
4888 lower inst.
(toned)

S₂

N₂
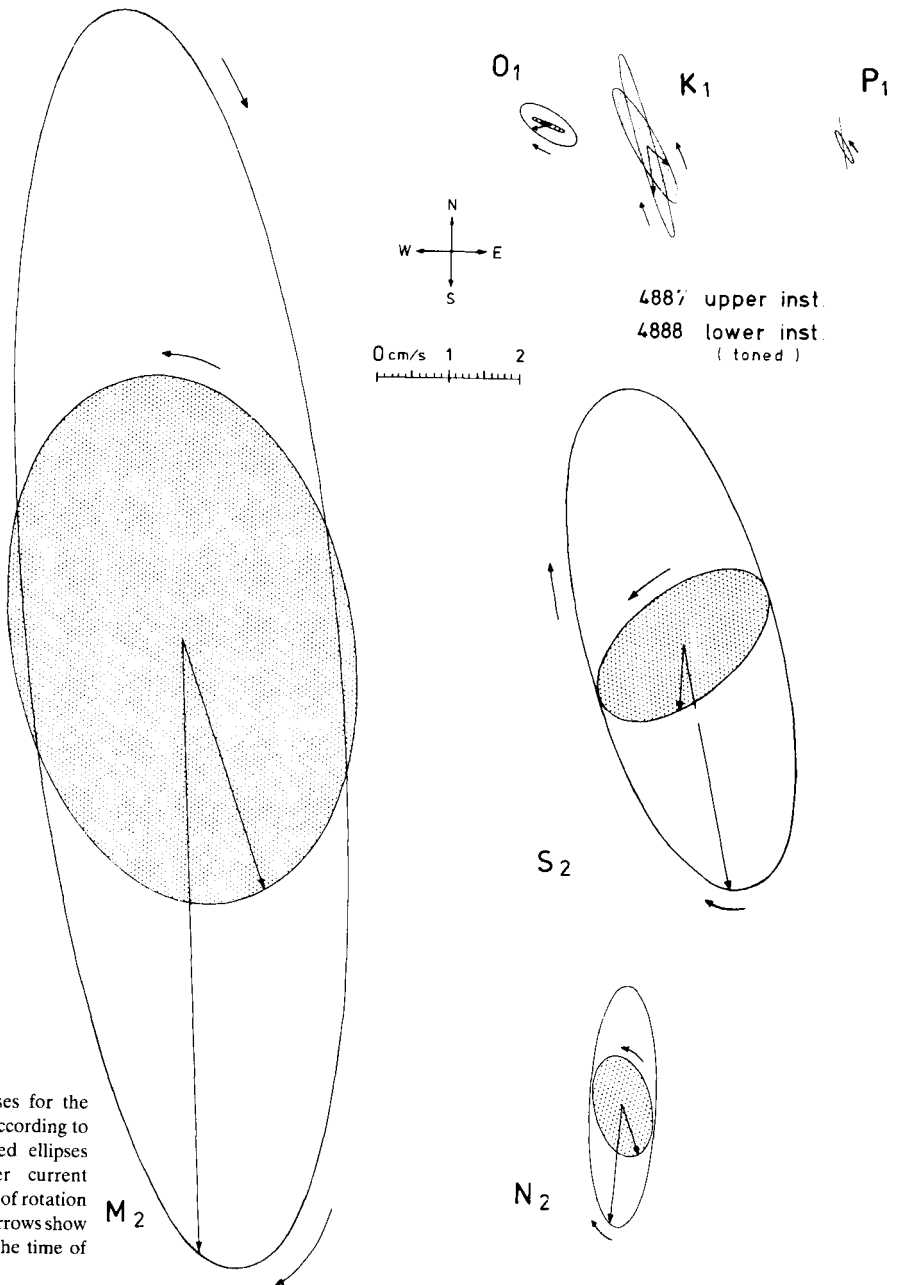
Fig. 10. Tidal ellipses for the major constituents according to Table 1. The shaded ellipses refer to the lower current meter. The direction of rotation is indicated and the arrows show the tidal current at the time of high water.

M₂